

# **INTERACTION OF HIGH INTENSITY LASER WITH STRUCTURED SNOW TARGETS**

**A.Zigler**  
**Hebrew University of Jerusalem**  
**Israel**

**2<sup>nd</sup>EAAC Workshop 2015**  
**Elba, Italy**

Collaborators :

M. Botton, Z.Henis, S. Eisenman, E.Nahum, I.

Pomerantz, E. Schleifer **Hebrew Univ. Jerusalem**

F. Abicht, J. Branzel, G.Priebe, M. Schnuerer

**Max Born Inst. Berlin**

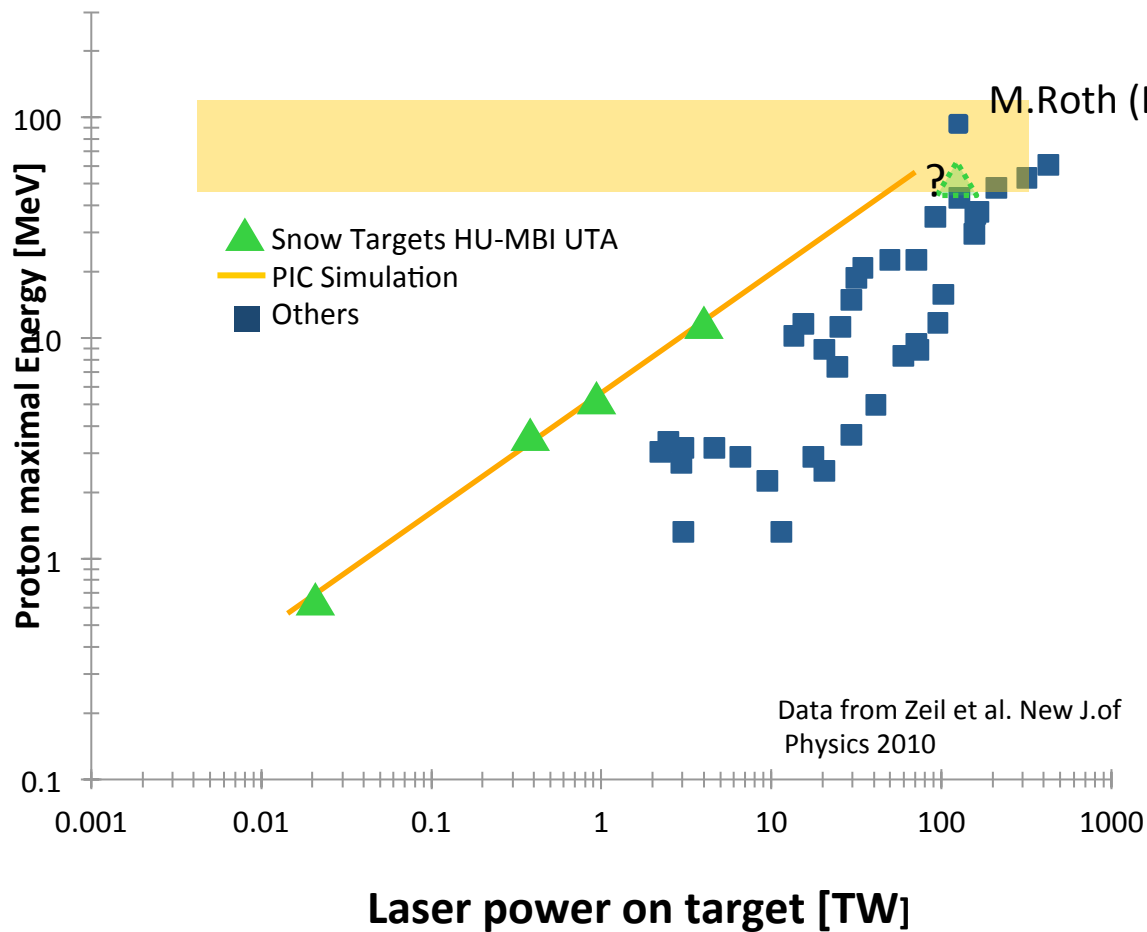
D. Gordon, P. Sprangle

**NRL Washington DC**

K.W.D.Ledingham

**Univ. Strathclyde  
Scotland**

# Proton energy vs. laser power (current status)



$$E_p \sim P_L^{1/2}$$

# Enhanced proton acceleration from snow (microwire) targets

The high proton energy can be attributed to several effects:

- The density gradient generated by the laser prepulse.
- Mass limited phenomenon.
- Localized field enhancement by the local plasma density near the tip of snow needle.
- Coulomb explosion of the positively charged snow needle, adding longtime acceleration of the protons.
- Aspect ratio of the needle.

# Highly structured snow surface

The snow is growing as pillars in the "normal" direction to the substrate.

The size of the snow pillars is highly non uniform and changes in the range of 30 -200  $\mu\text{m}$ .

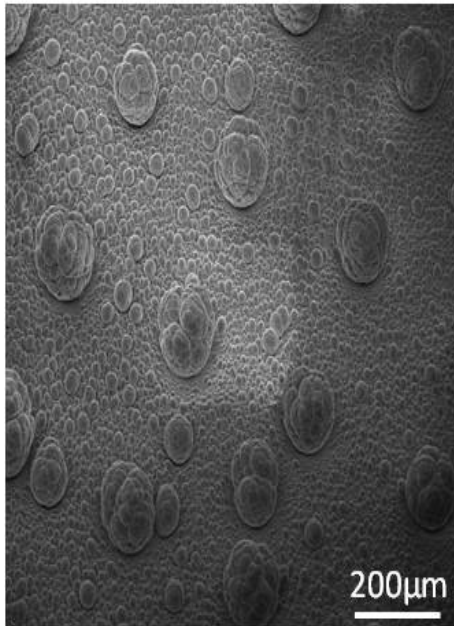
The aspect ratio of the pillars decreases as the scale size decreases. The smallest features, spatially resolved, are with diameter about 0.5 - 2  $\mu\text{m}$

The surface can be characterized by three roughness scales:

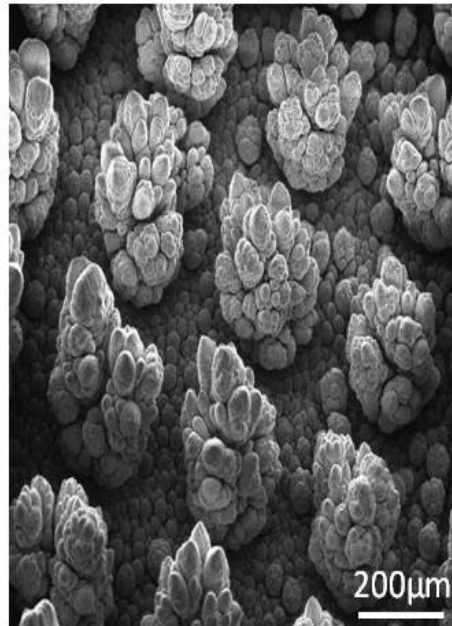
- a) pillars of about 100  $\mu\text{m}$
- b) spikes of about 10  $\mu\text{m}$  on top of them
- c) whiskers of about 1  $\mu\text{m}$  on the spikes.

# Control of the structured snow target by changing the flow rate and varying the nucleation centers

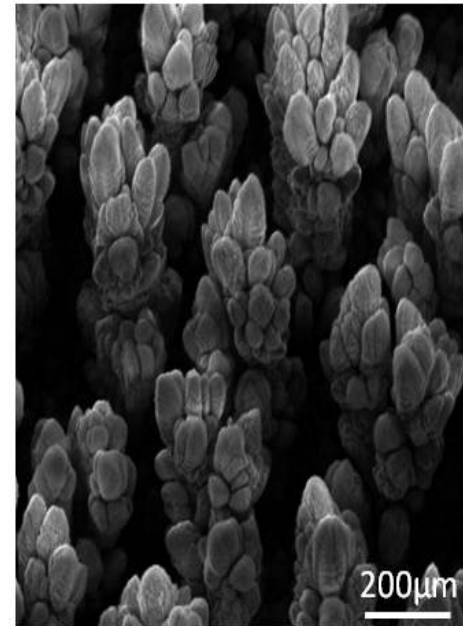
Flow 0.9 SCFH  
TIME 480 SEC



Flow 1.75 SCFH  
TIME 240 SEC



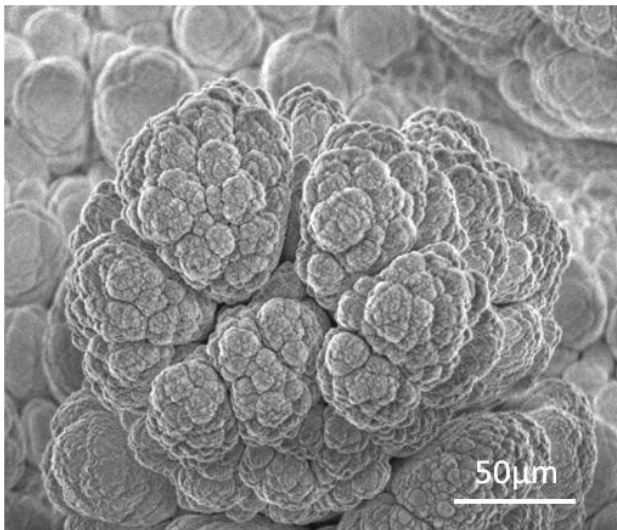
Flow 3 SCFH  
TIME 80 SEC



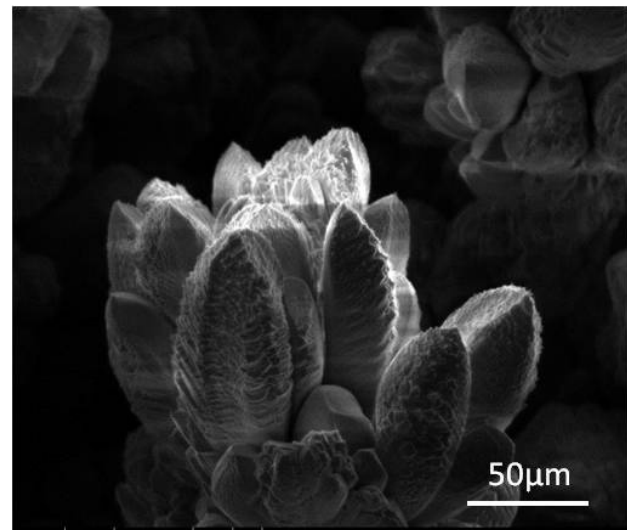
**SEM images of snow pillars that were grown over artificial Aluminum nucleation centers on Sapphire substrate at various growth conditions.**

# Control of morphology by growth kinetics

0.9 SCFH, 480 sec



3 SCFH, 80 sec

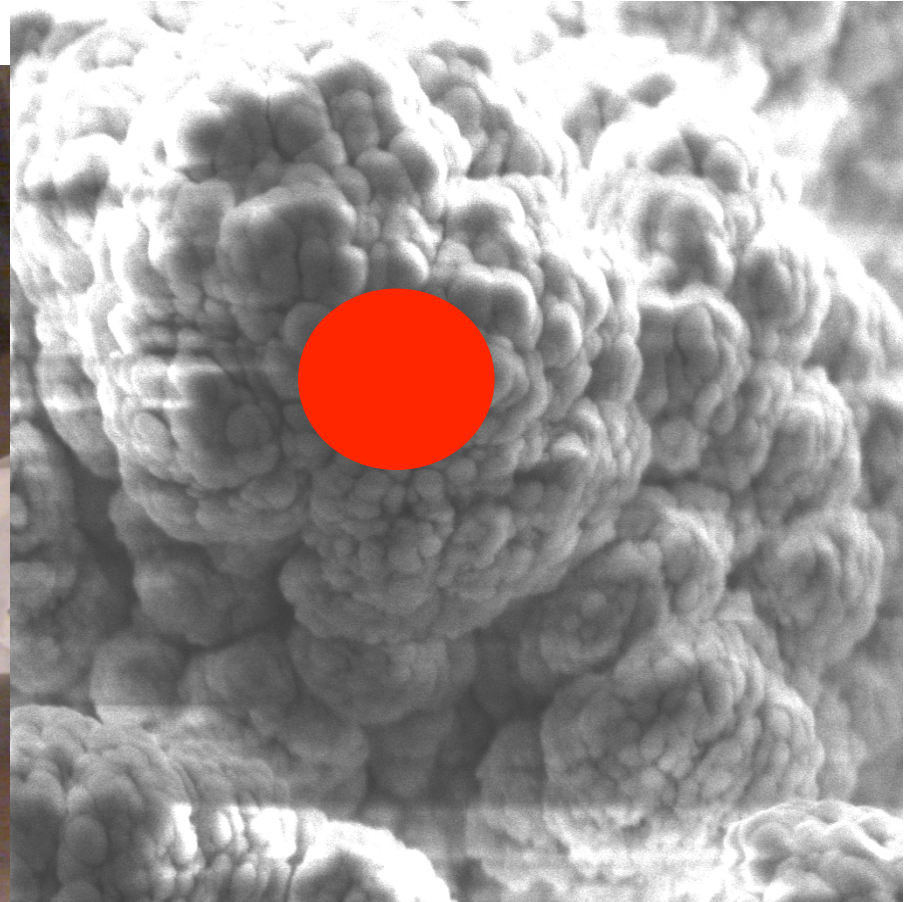


# Snow target In the ESEM



HV	Mag	WD	Spot	Sig
5.0 kV	1000x	16.23 mm	4.0	SE

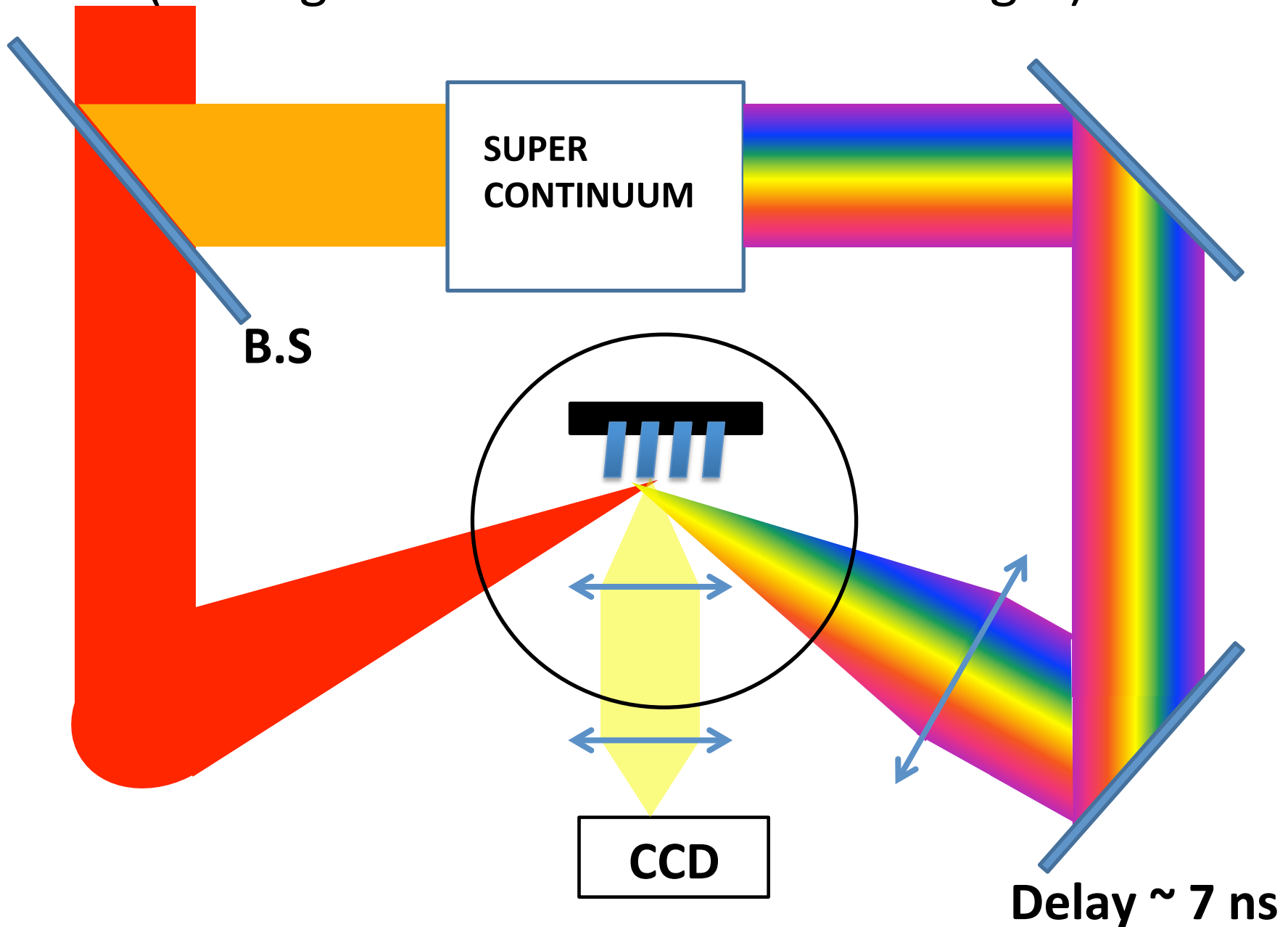
50  $\mu$ m



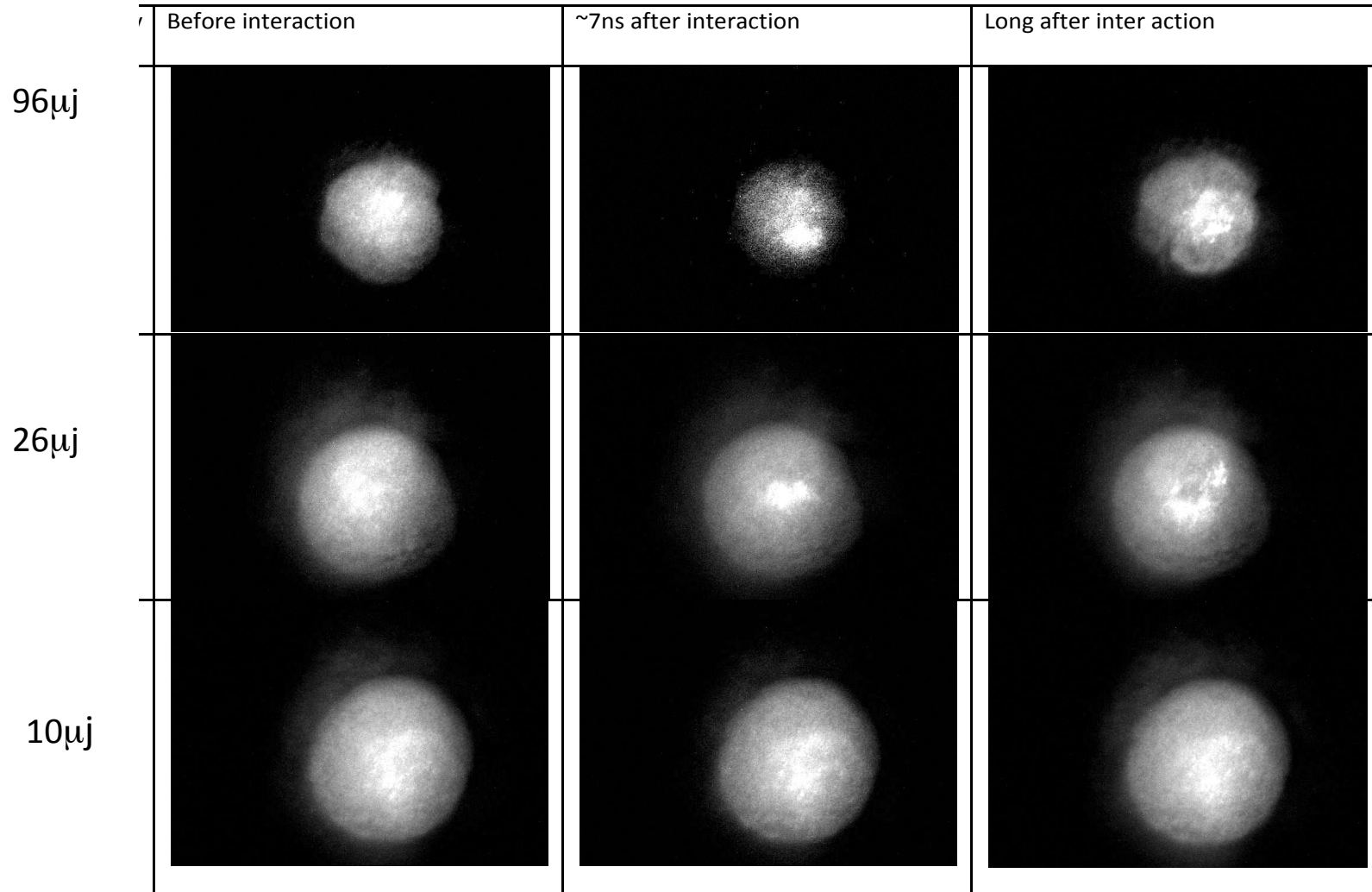
HV	Mag	WD	Spot	Sig
5.0 kV	12000x	5.82 mm	4.0	SE

5  $\mu$ m

# Influence of the pre pulse (damage threshold of the snow target)



LASER @ ~70 fsec. Field of view 400x300  $\mu\text{m}$ . Just Strobe images.

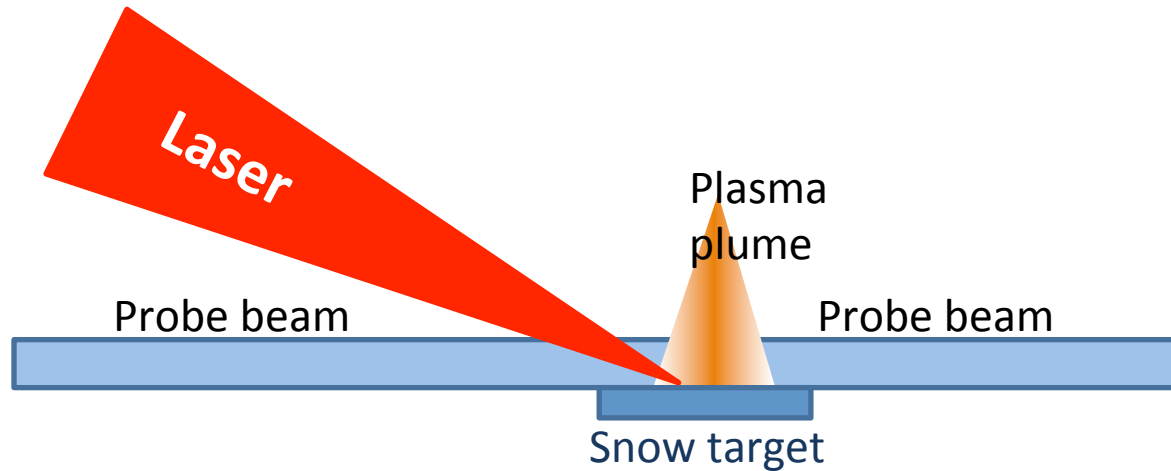


The damage threshold –  $0.3\text{j}/\text{cm}^2$



**Less than 1 microjoule for tight (<10 micron) focusing !**

# Pre-plasma density spatial profile

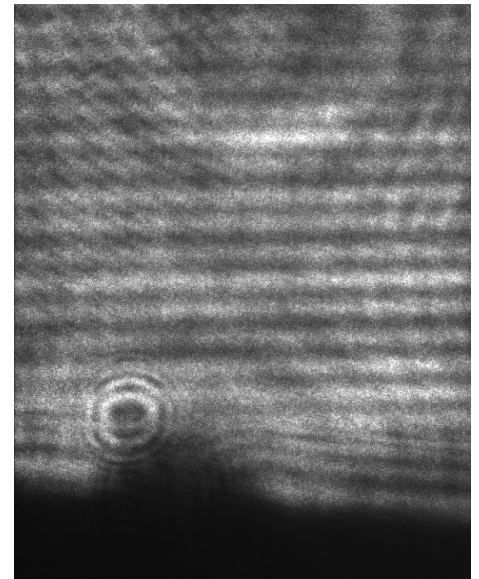


Lloyd mirror  
interferometry  
and schlieren  
shadowgraphy

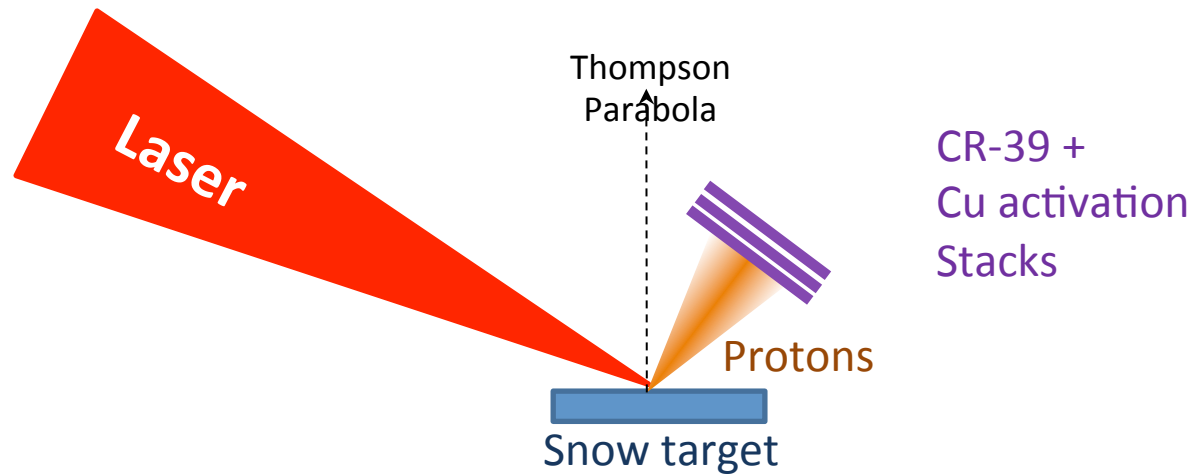
Interferometry Measurements:

Electron density up to  $N_e \sim 10^{20} \text{ cm}^{-3}$

Spatial resolution up to 1-3 microns

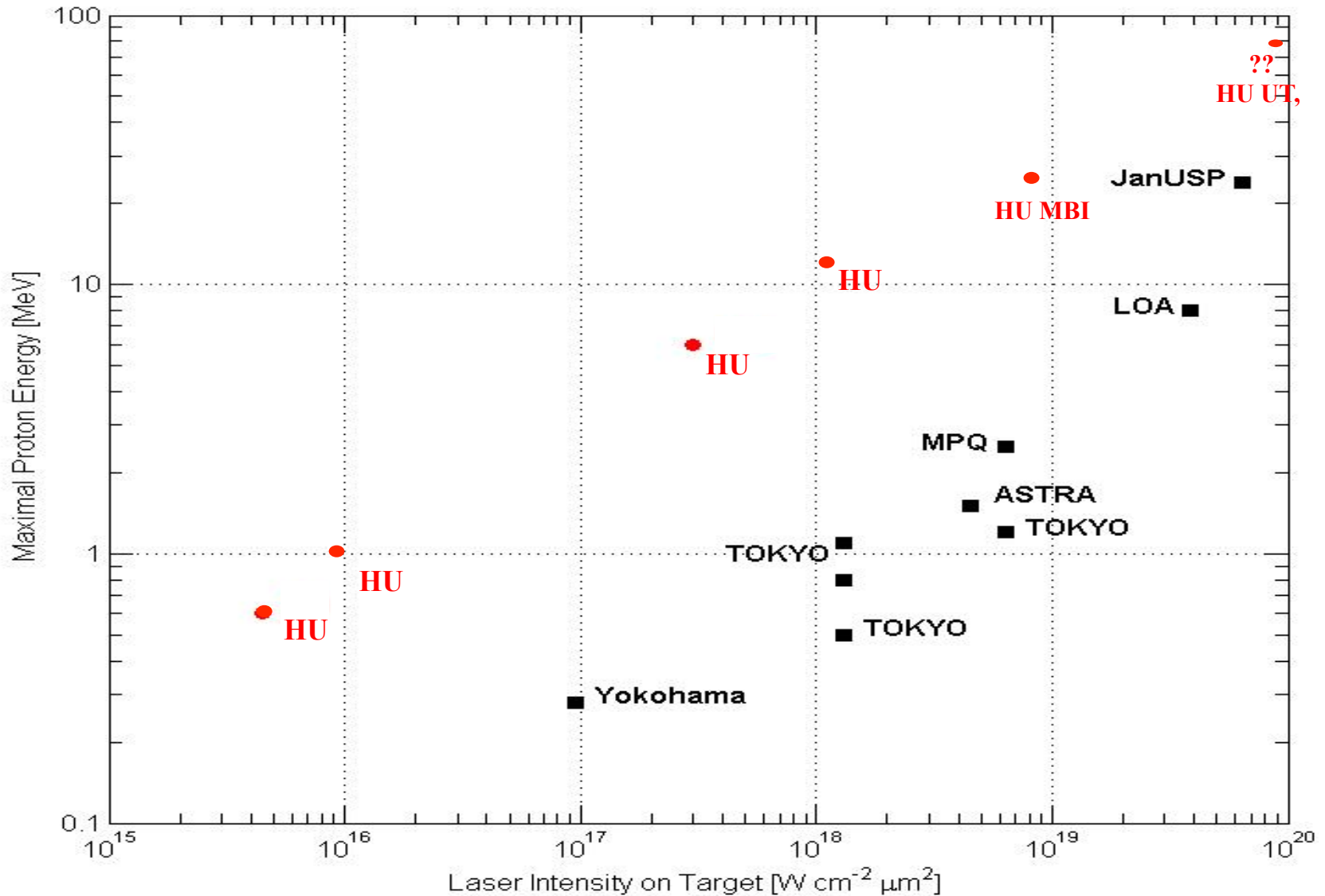


# Experimental Setup



Laser Parameters	HU	MBI (up to 10TW on target in or exper.)	Texas PTW (40TW on target in our experiment)
Energy (on target)	50 mJ	400 mJ	100 J
Pulse Duration	50 fsec	65 fsec	150fsec
Spot Size	10 $\mu\text{m}^2$	10 $\mu\text{m}^2$	10 $\mu\text{m}^2$ (multi spots)
Contrast Ratio	$10^{-4}$ (10 nsec)	$10^{-5}$ (6 nsec) (artificial pre-pulse)	$10^{-6}$ (100 nsec ,many prepulses) $10^{-8}$ (with plasma mirror)

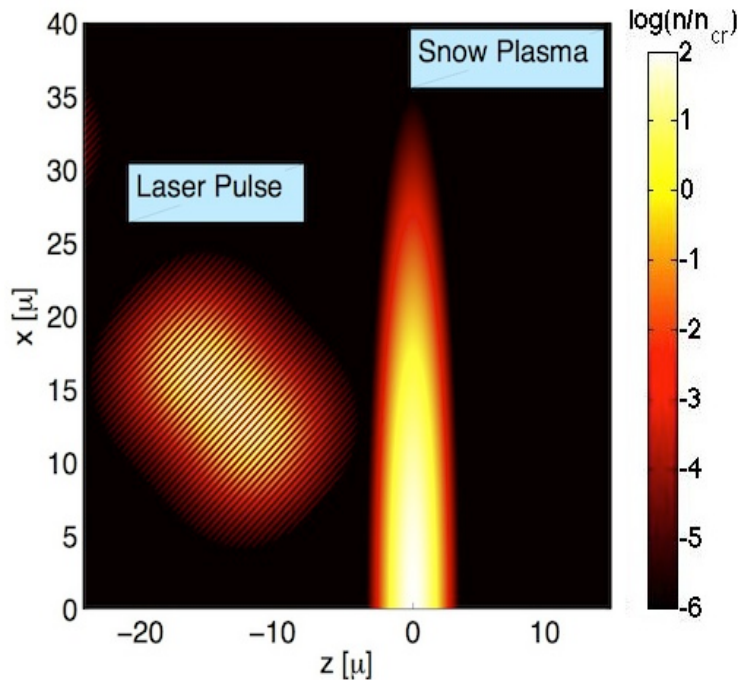
# Max Proton Energy vs. Intensity



# Model of laser whisker interaction

- Interaction of the laser with a single wire.
- The prepulse with the same time duration as the main pulse generates plasma with temperature of 2–5 eV.
- During the 10 ns interval between the prepulse and the main pulse the plasma expands forming a cylindrical plasma column.
- The main pulse interacts with a proper density scale length plasma.

# Laser – snow wire interaction by 2D PIC simulations with TURBOWAVE



Laser: 88 fs (32 + 24 + 32),  
0.8  $\mu\text{m}$ , 4-5  $\mu\text{m}$  spot size,  
 $2.5 \cdot 10^{17} - 2.5 \cdot 10^{19}$  W/cm<sup>2</sup>

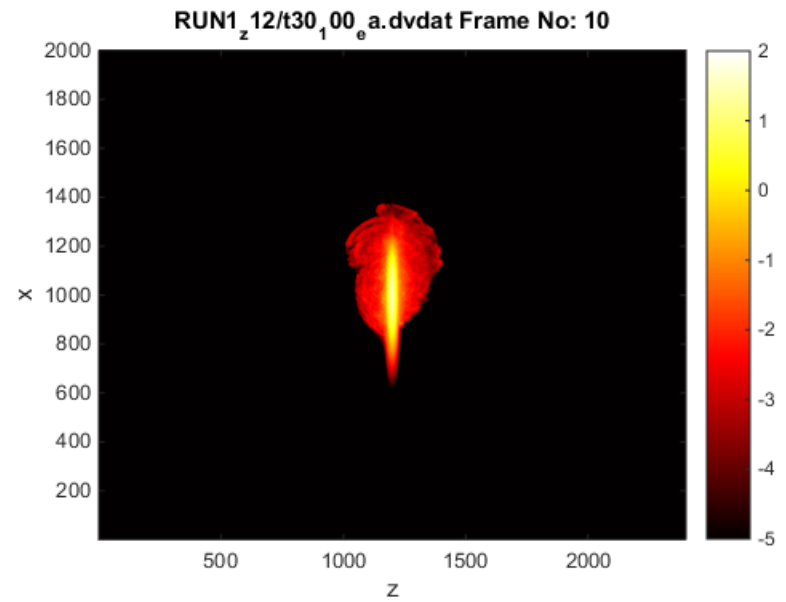
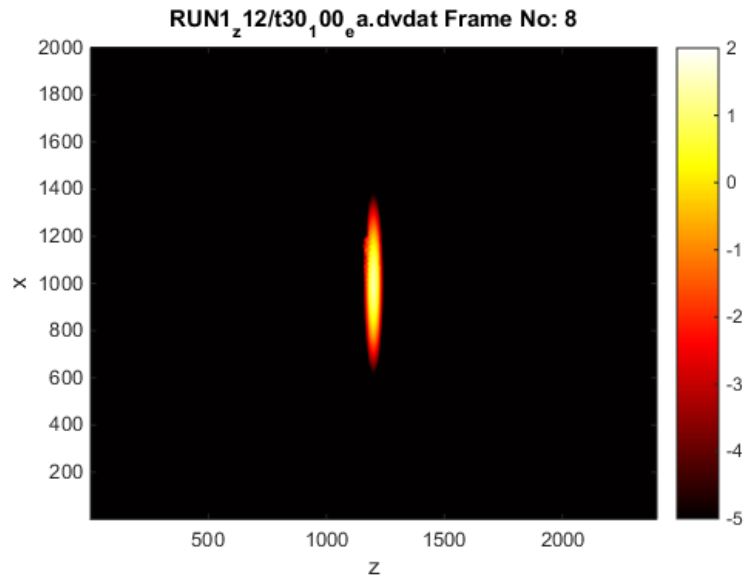
The core of  $100 \cdot n_{cr}$  : ellipsoid  $\sim 0.1\text{-}0.2\mu\text{m} \times 1\text{-}2\mu\text{m}$  .  
The critical density contour: ellipsoid  $\sim 1\text{-}2\mu\text{m} \times 10\mu\text{m}$  .

# Acceleration process

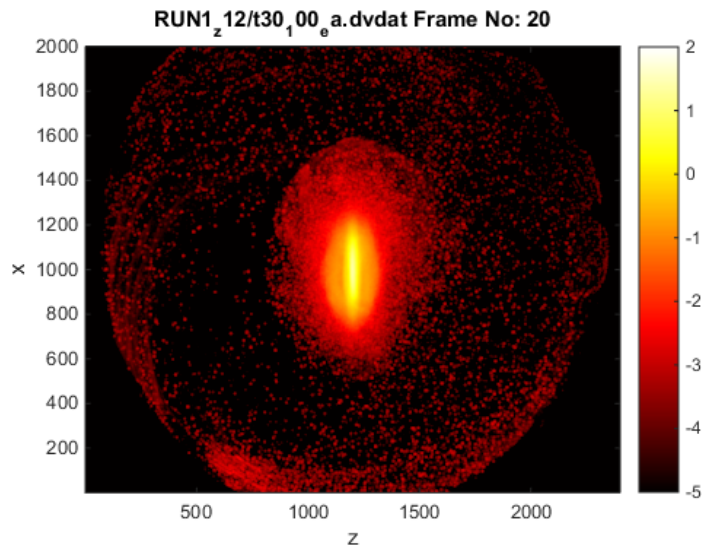
- Electrons are driven out of the plasma ellipsoid, starting charge separation  $\sim \tau_L$ . Unlike TNSA, no difference between front and rear surface.
- After passage of the laser, electrons accumulate near the tip, the protons start to react,  $\sim (2 - 3) \tau_L$ .
- The electrons accumulation near the tip is reduced, charge separation still maintained,  $(3 - 6) \tau_L$ . Oxygen ions add a pushing field.
- Late times, acceleration ceases, the protons move at constant velocity.

# Electrons

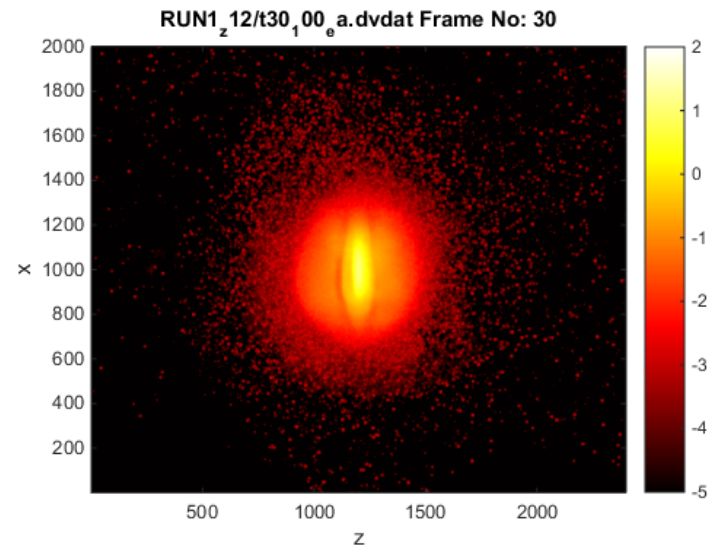
## 36 fs



## 212 fs



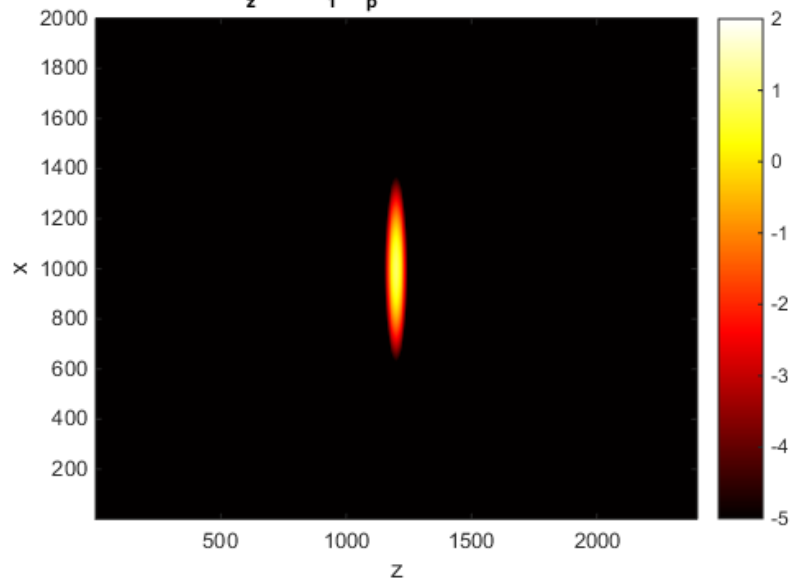
## 390 fs



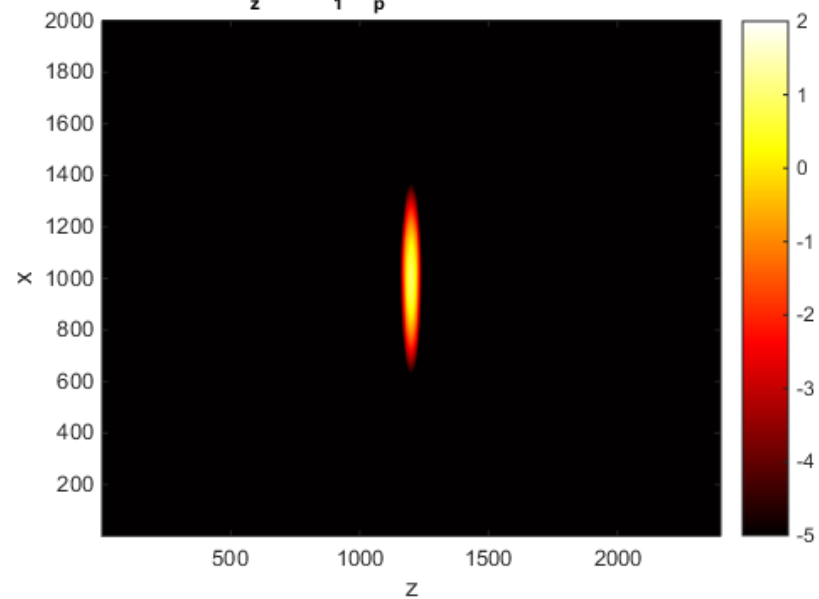
# Protons

## 36 fs

RUN1\_z12/t30\_1\_00\_p.a.dvdat Frame No: 8

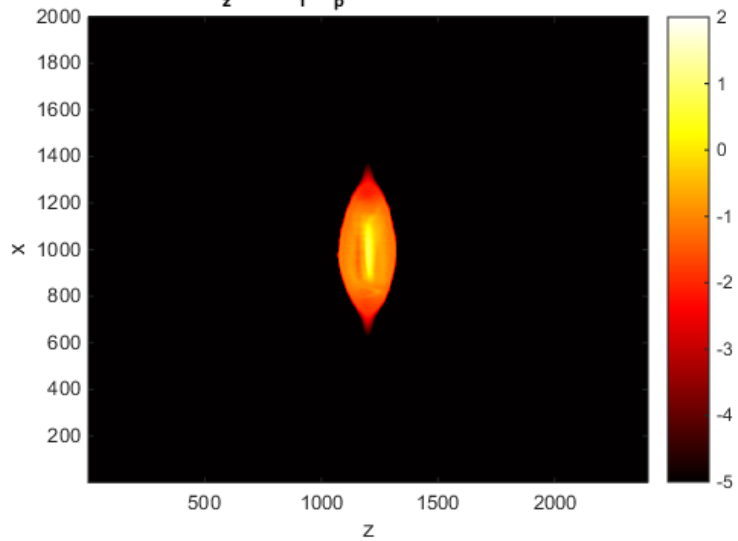


RUN1\_z12/t30\_1\_00\_p.a.dvdat Frame No: 10



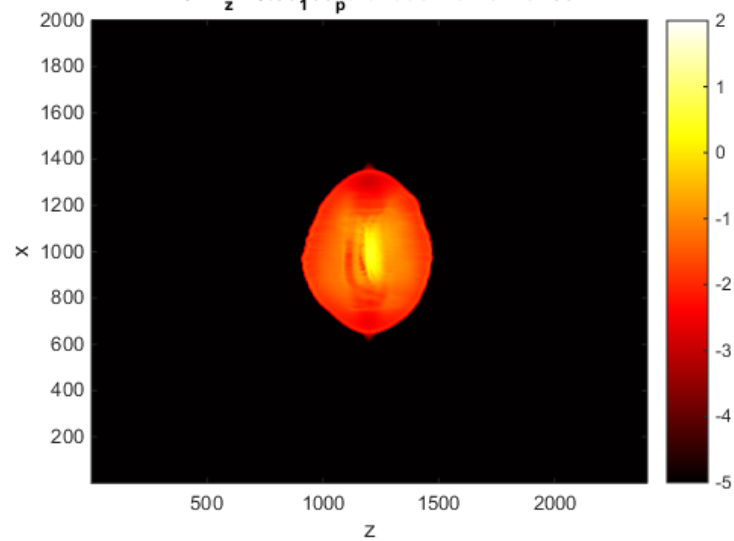
## 212 fs

RUN1\_z12/t30\_1\_00\_p.a.dvdat Frame No: 20



## 390 fs

RUN1\_z12/t30\_1\_00\_p.a.dvdat Frame No: 30

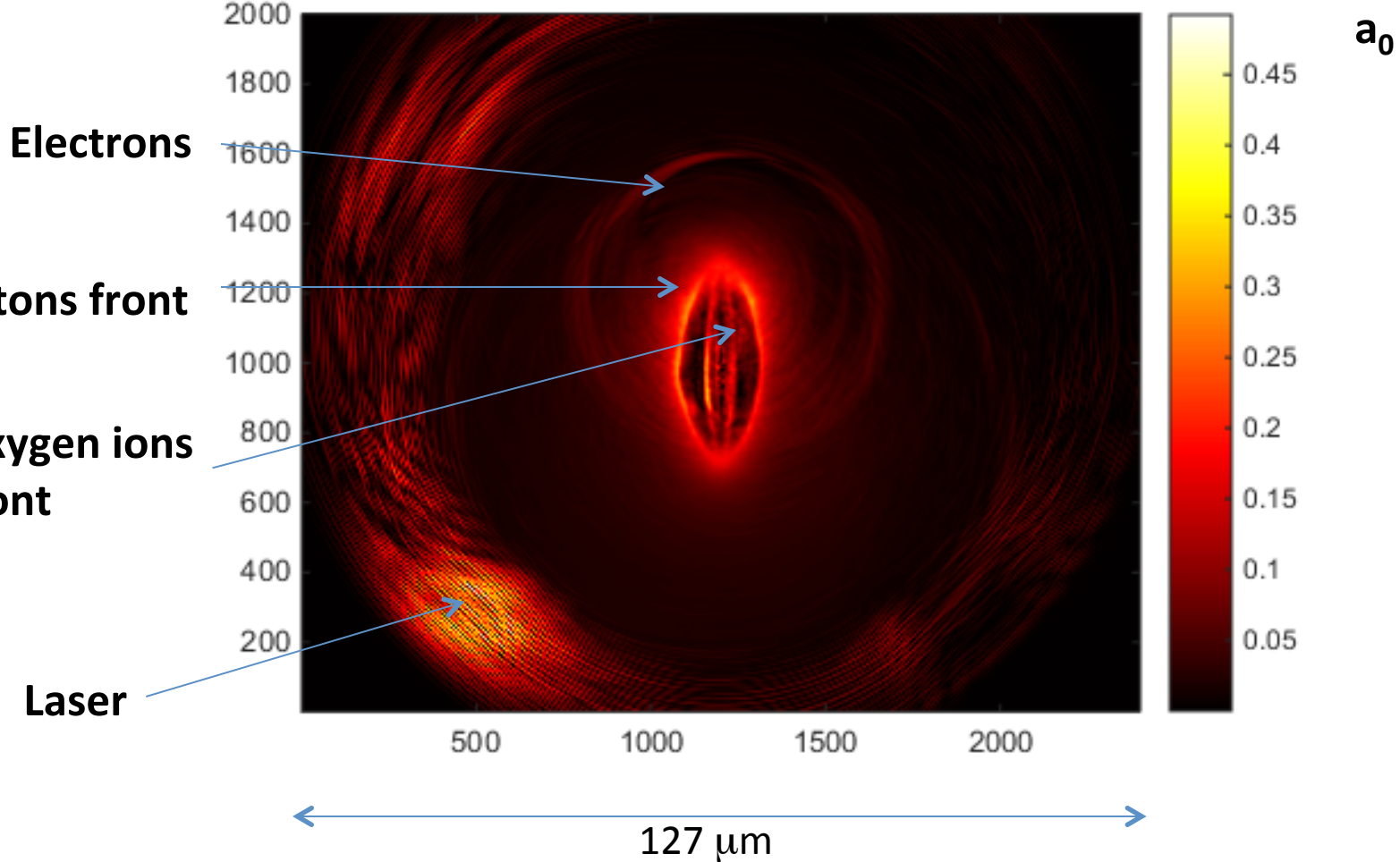


# The electric field in units of $a_0$

( $\times 1.37 \cdot 10^{11}$  V/cm)  $I_L = 2.5 \cdot 10^{19}$  W/cm<sup>2</sup>

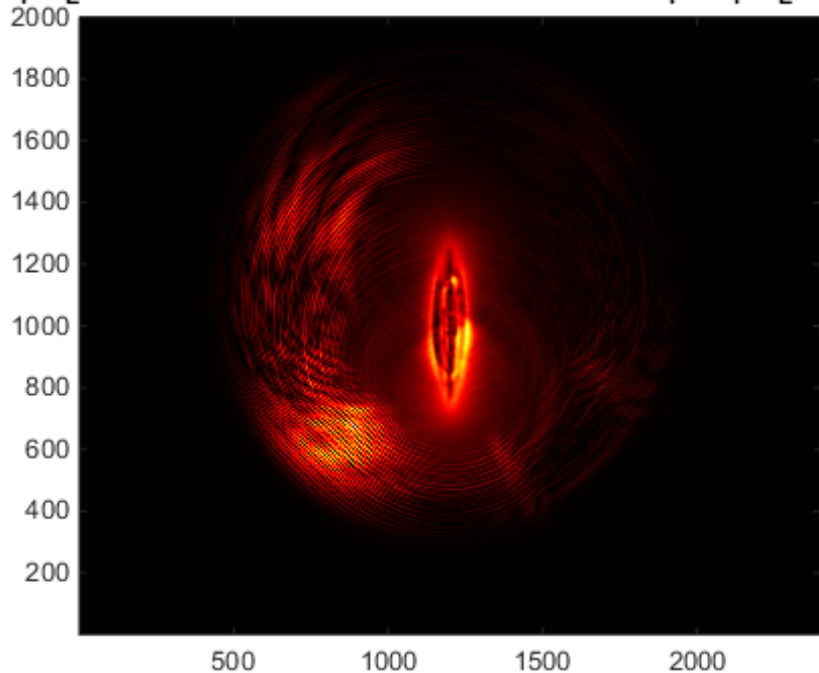
$$a_0 = \frac{eE}{mc\omega}$$

1\_1/t30\_1\_00\_E.x.dvdat Frame No: 20 qudadd G2N2L2O1\_1/t30\_1\_00\_E.z.dvdat Frame No:



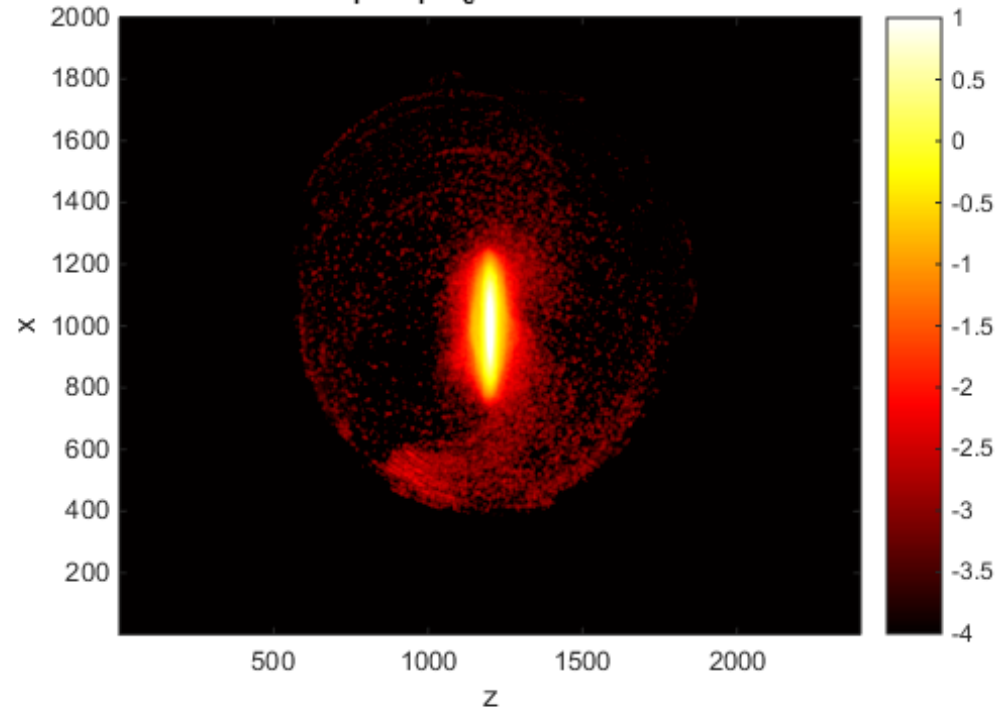
# The electric field at times shorter than 2-3 times the laser pulse duration is dominated by the electrons cloud

30\_00\_E\_x.dvdat Frame No: 15 qudadd G2N2L2O1\_1/t30\_00\_E\_z.dv



Electric field in  $a_0$

G2N2L2O1\_1/t30\_00\_e.a.dvdat Frame No: 15

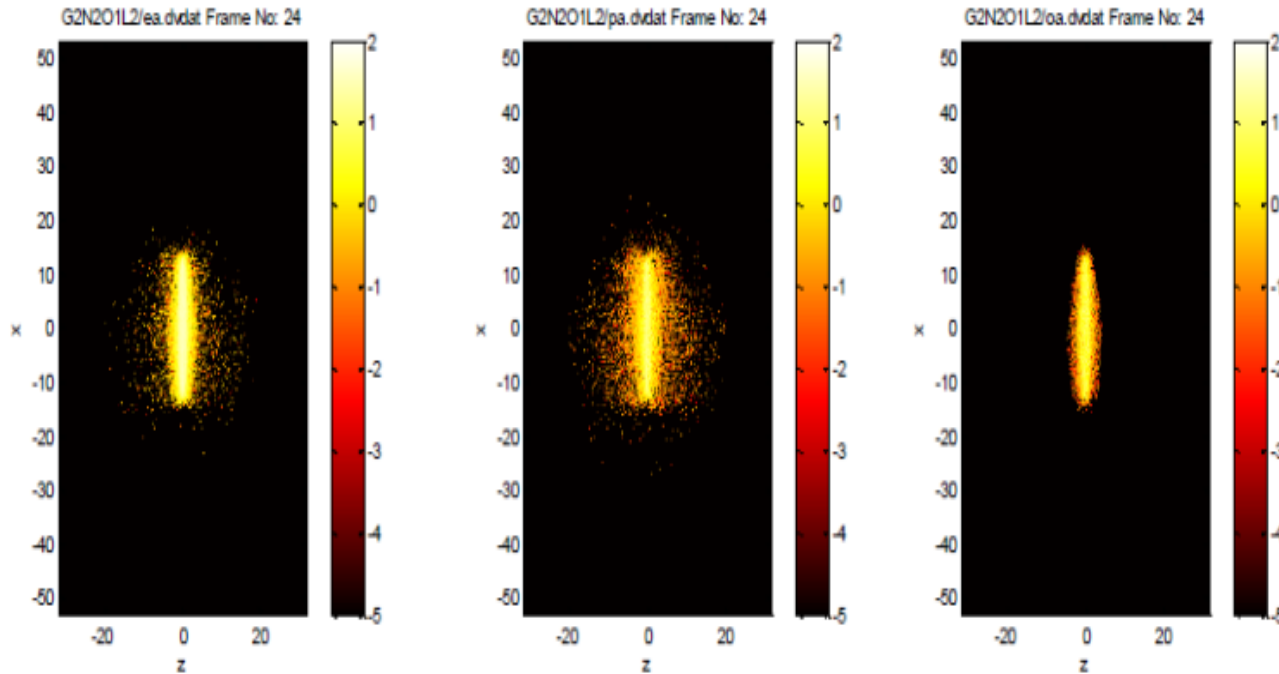


← 127  $\mu\text{m}$  →

Electrons spatial distribution



# Constant solid density



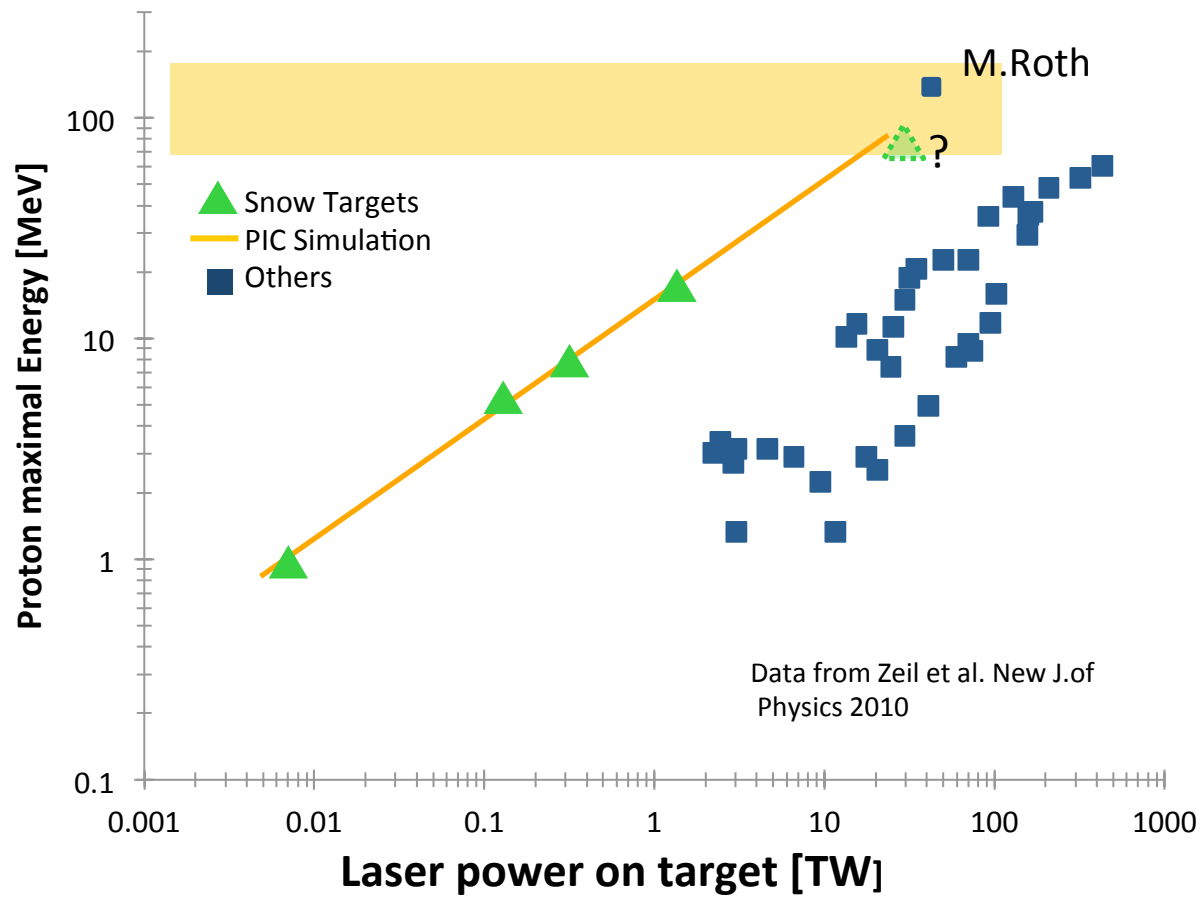
Electrons

Protons

Oxygen

$I_L = 2.5 \cdot 10^{19} \text{ W/cm}^2$ , propagating at  $45^\circ$  relatively to the whisker major axis.  
Time = 672 fs after the laser pulse hit the whiskers.

# Proton energy vs. Laser power



Thank you

# Output of 1D model - accelerated protons energy

- Field enhancement:  $a_{0\text{eff}} \sim 3a_0$

- Hot electrons:  $k_B T_h = m_e c^2 \left[ \sqrt{1 + \frac{I \lambda^2}{1.37 \cdot 10^{18}}} - 1 \right]$

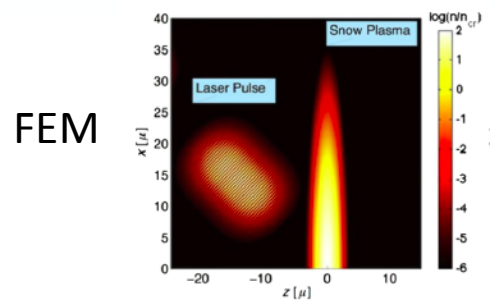
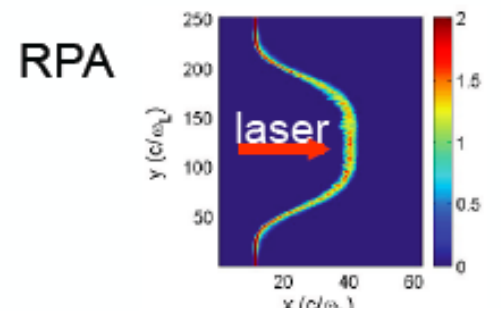
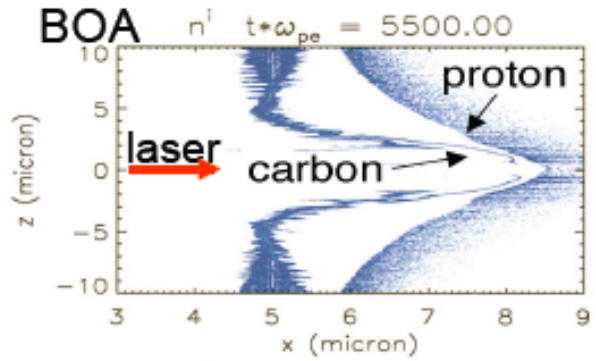
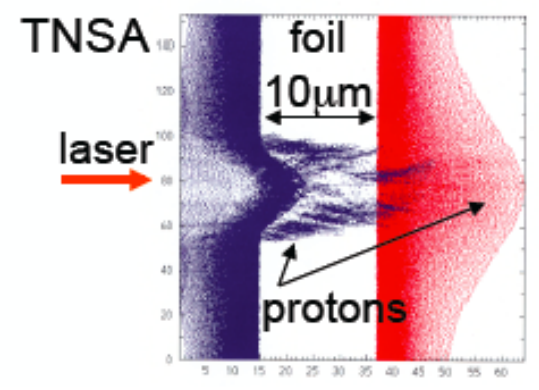
- Short length scale:  $L \sim 0.05 \lambda$

- Accelerating field:  $E_{\text{acc}} \approx \frac{kT_{\text{hot}}}{eL}$

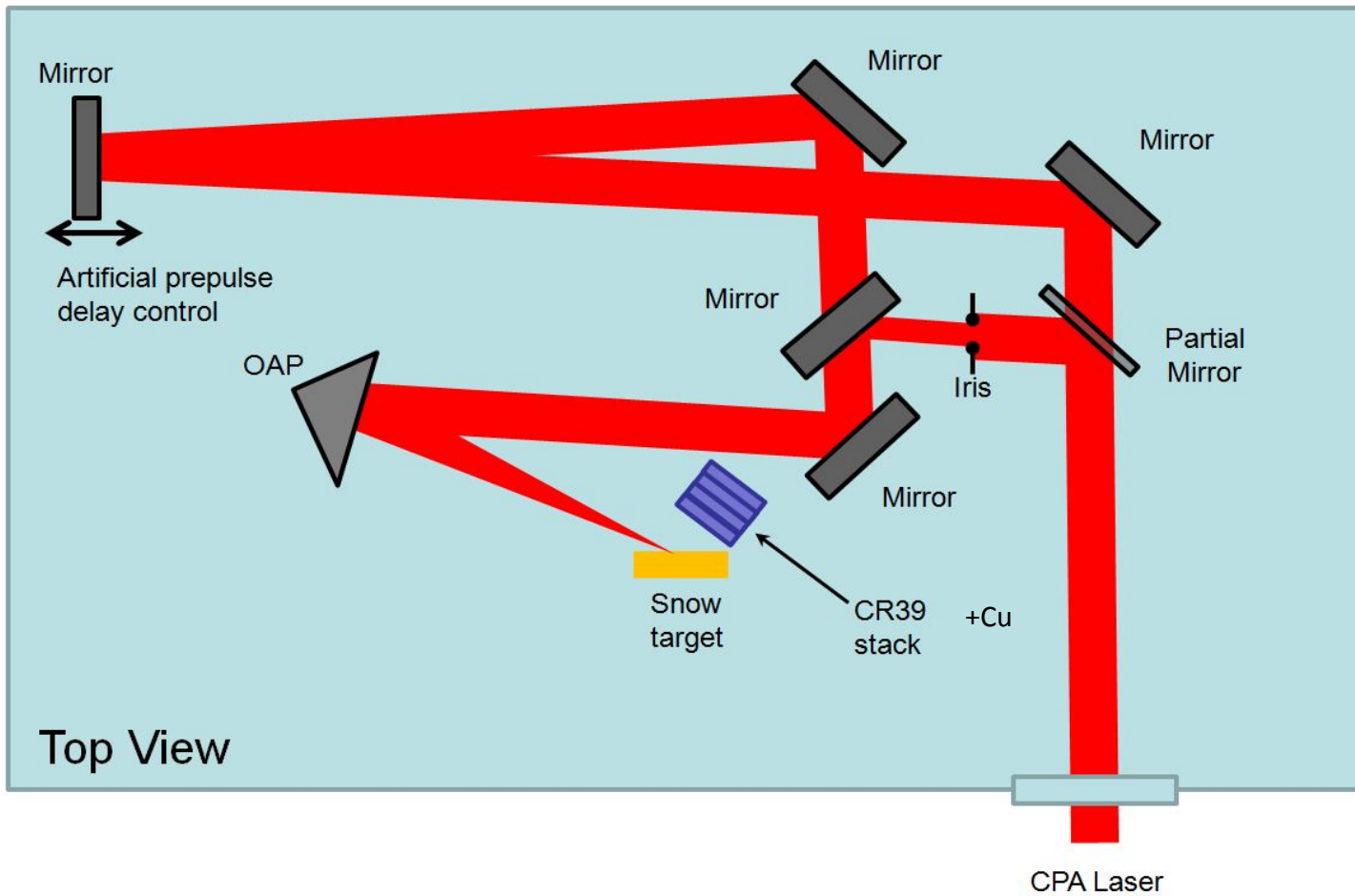
- Ion energy: accelerated along one wavelength

$$E_{\text{proton}} \cong E_{\text{acc}} \times \lambda = 20kT_{\text{hot}} = 6\text{MeV} \quad \text{At } k_B T_h \sim 300 \text{ keV}$$

Ion acceleration mechanism	Acronym	Ion Accel. process
Target-Normal Sheath Acceleration <i>S. Hatchett et al., Phys. Plas. 7, 2076 (2000)</i>	TNSA	Charge separation  GeV protons? <b>X</b>
Break out afterburner <i>L. Yin et al., Laser Part. Beams 24, 291 (2006) ; Phys. Plasmas 14, 056706 (2007)</i>	BOA	Kinetic Process (Buneman): relative e-i drift GeV protons? <b>✓</b> Linear Polar.
Radiation Pressure Acceleration, Aka Plasma Piston <i>E.g., A.P.L. Robinson, et al., New J. Phys. 10, 013021 (2008)</i>	RPA	Charge separation  GeV protons? <b>✓</b> Circular Polar.
Field Enhancement by Microwires <i>Zigler et al PRL 2013</i>	FEM	Charge separation 150 MeV protons by 200 TW



# Experiments of proton acceleration with snow targets



# Shot 7354 Texas PW (42TW on Target)

- AR plasma mirrors slides
- Stack (protons arrive from the left):



- Geiger counter - Cu#1 signal

# Cu Activation (TU)

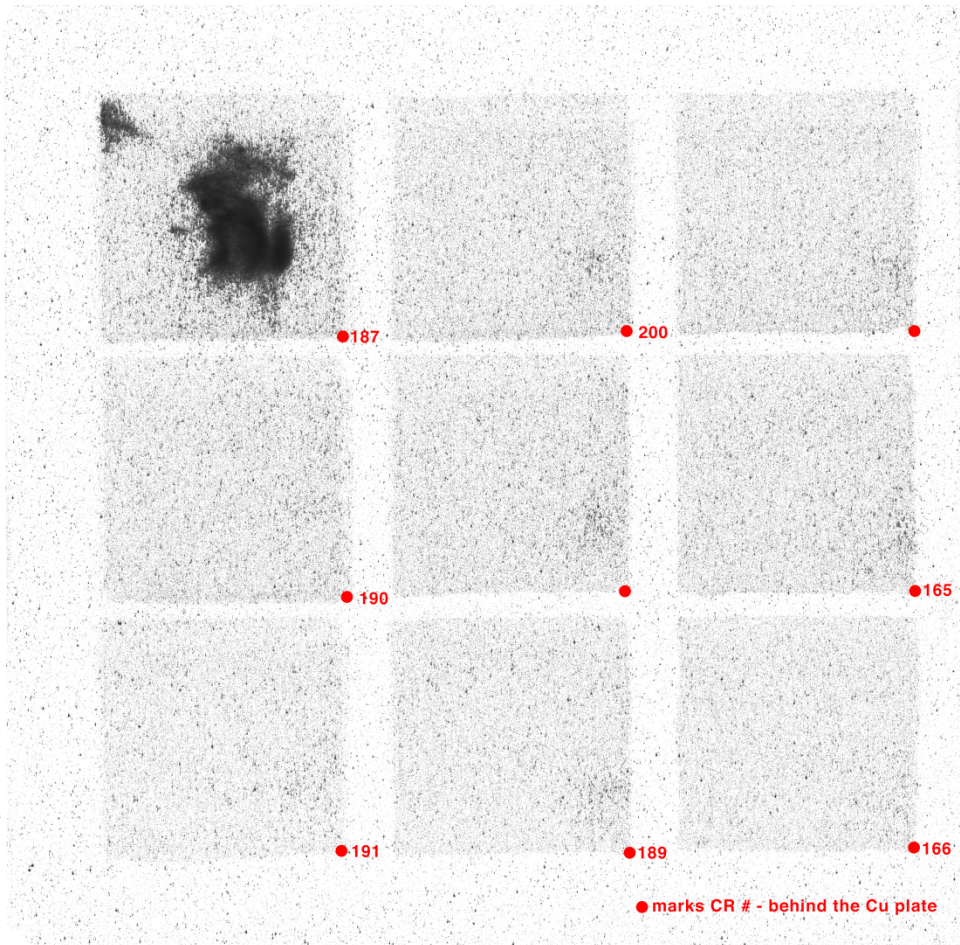


Image plate scan (with grey level adjusted)

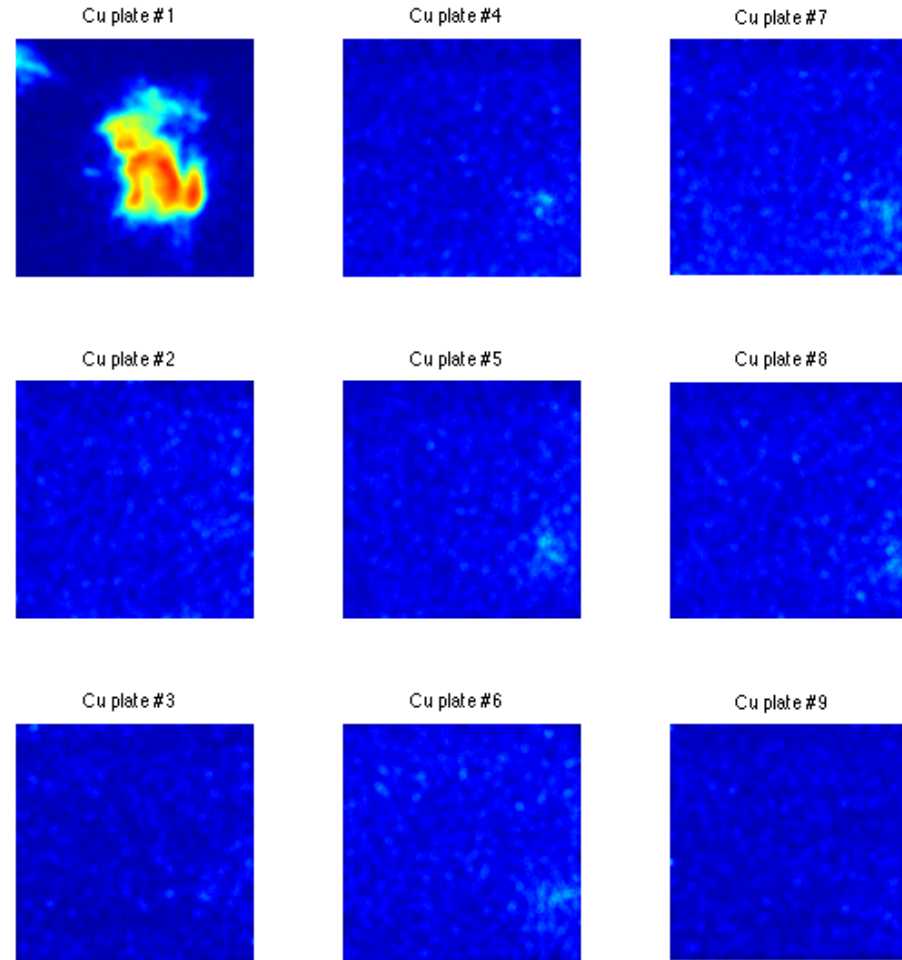
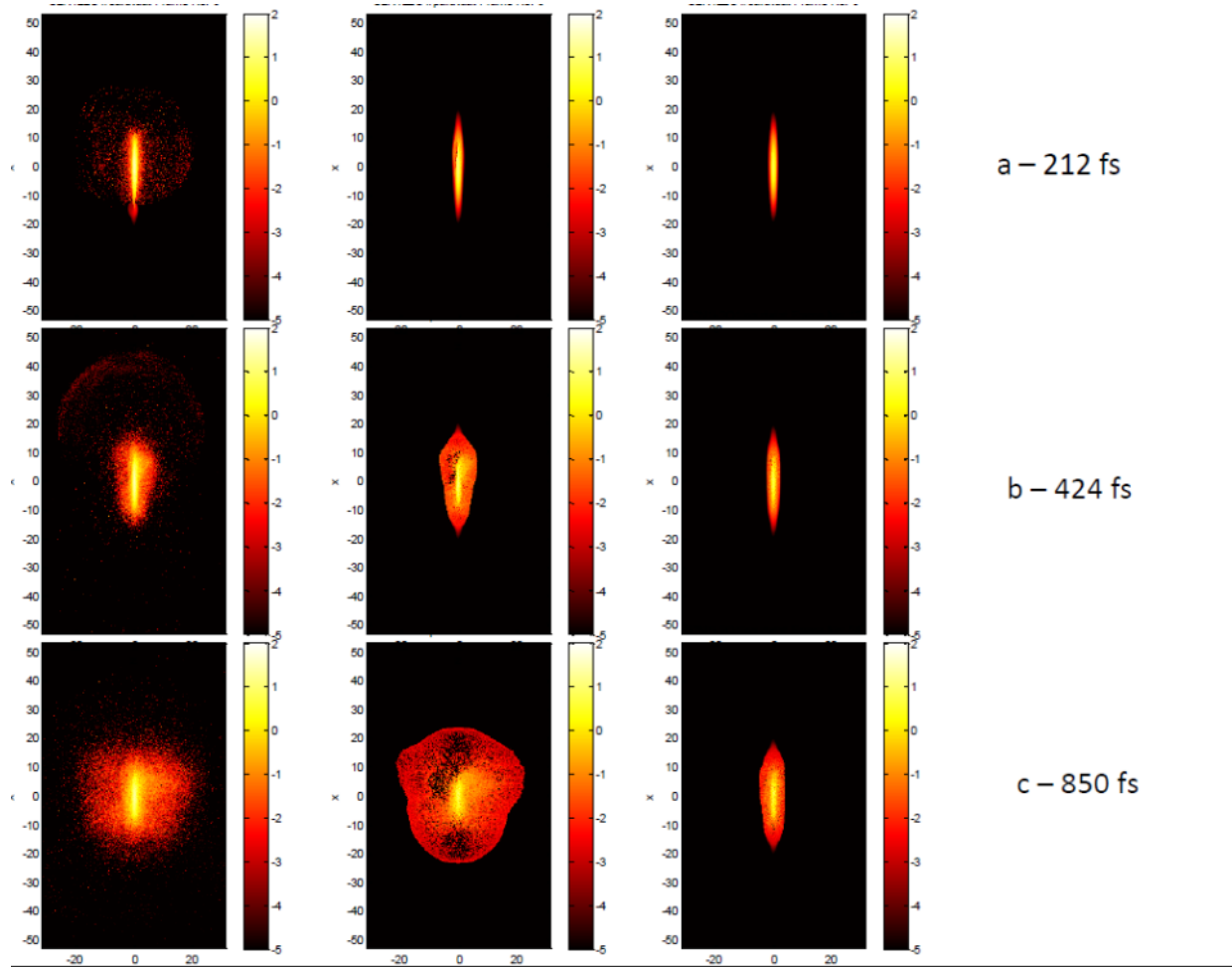


Image plate scan (with spatial 1mm average)

$I_L = 2.5 \cdot 10^{19} \text{ W/cm}^2$ ,  $90^\circ$  irradiance, at 141 fs.

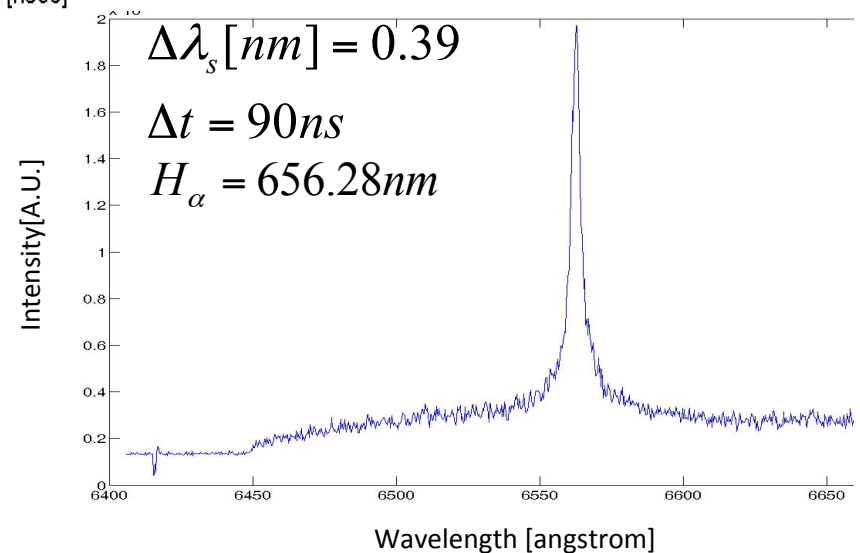
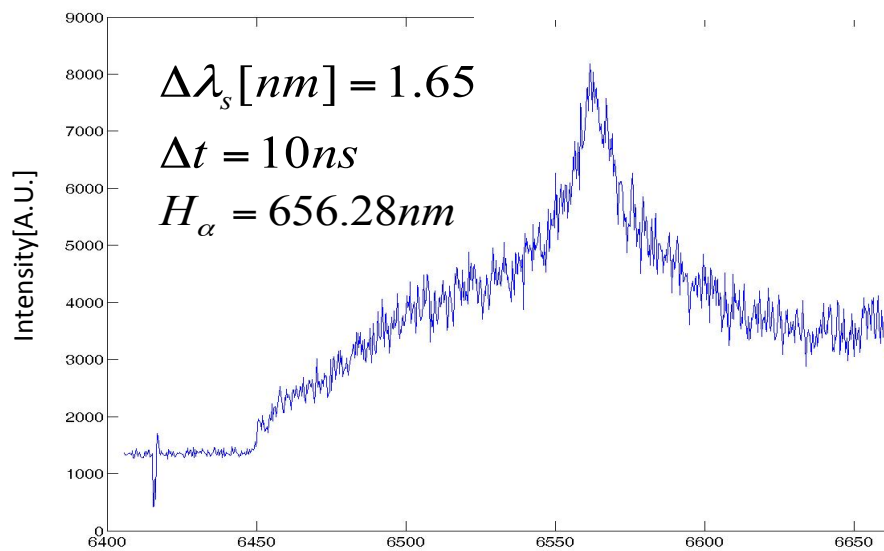
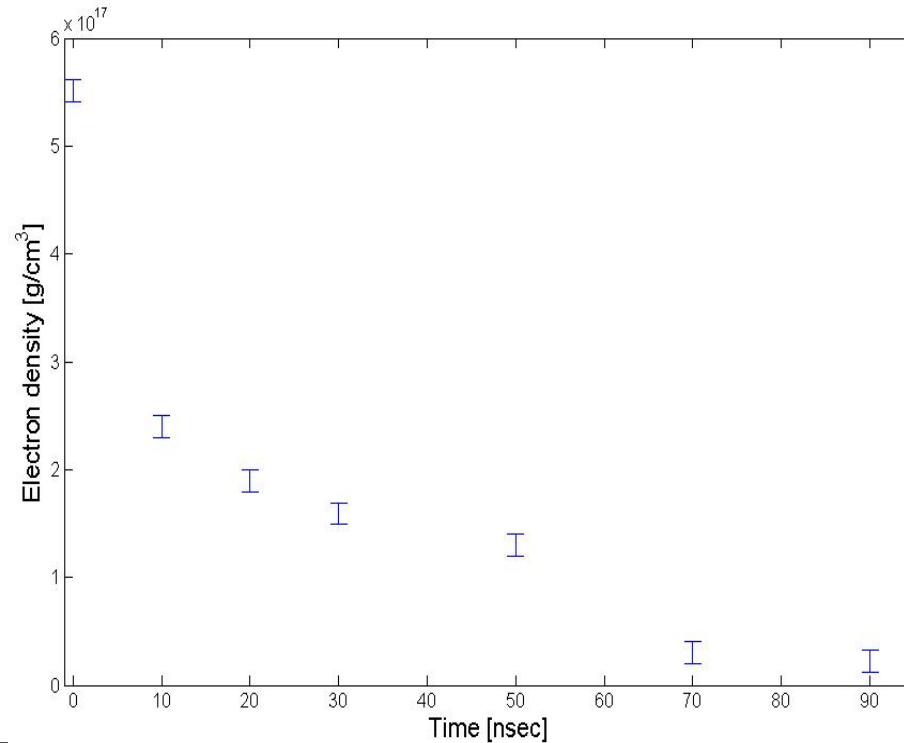


Electrons

Protons

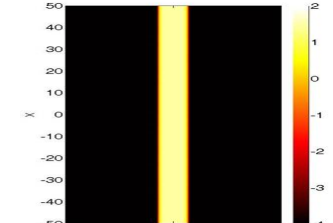
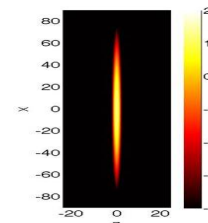
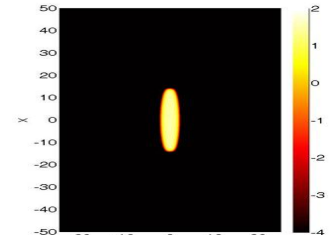
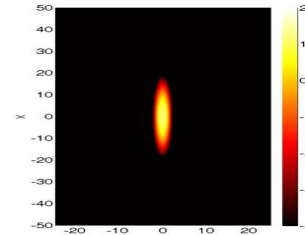
Oxygen

# Pre-plasma density temporal profile



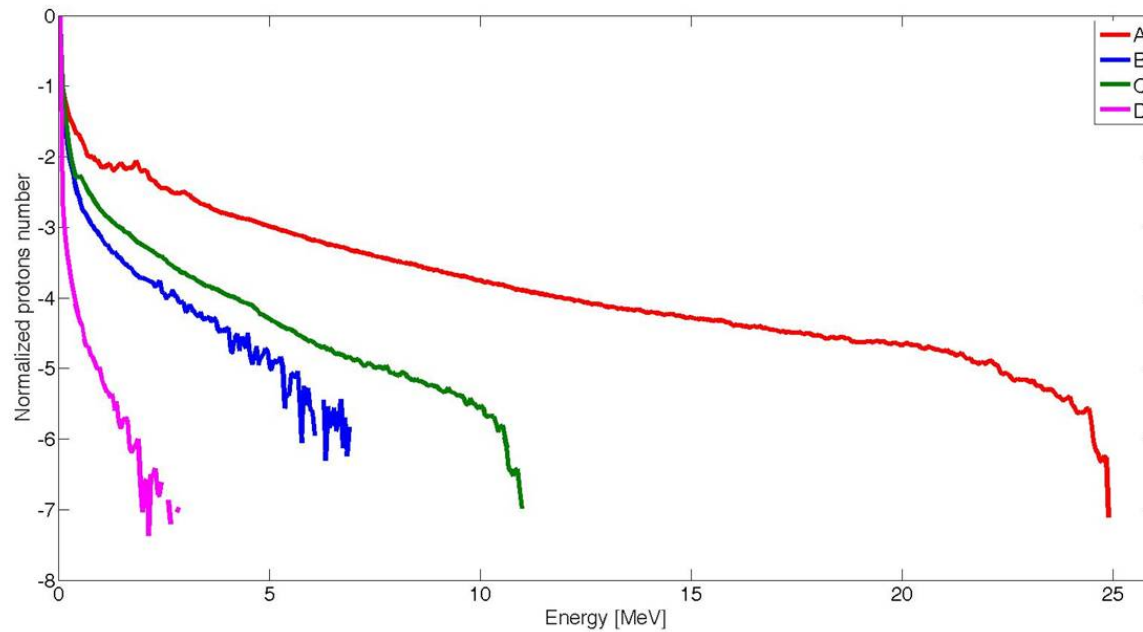
# Protons energy spectrum

$I_L = 2.5 \cdot 10^{19} \text{ W/cm}^2$ ,  
propagating at  $45^\circ$ .



C

D



# Collisionless plasma description

$$\left\{ \begin{array}{l} \frac{\partial f_j}{\partial t} = -\mathbf{v} \cdot \frac{\partial f_j}{\partial \mathbf{x}} - q_j \left( \mathbf{E} + \frac{\mathbf{v}}{c} \times \mathbf{B} \right) \cdot \frac{\partial f_j}{\partial \mathbf{p}} \\ \nabla \cdot \mathbf{E} = 4\pi\rho \\ \nabla \times \mathbf{E} = -\frac{1}{c} \frac{\partial \mathbf{B}}{\partial t} \\ \nabla \times \mathbf{B} = \frac{4\pi}{c} \mathbf{J} + \frac{1}{c} \frac{\partial \mathbf{E}}{\partial t} \\ \nabla \cdot \mathbf{B} = 0 \end{array} \right.$$

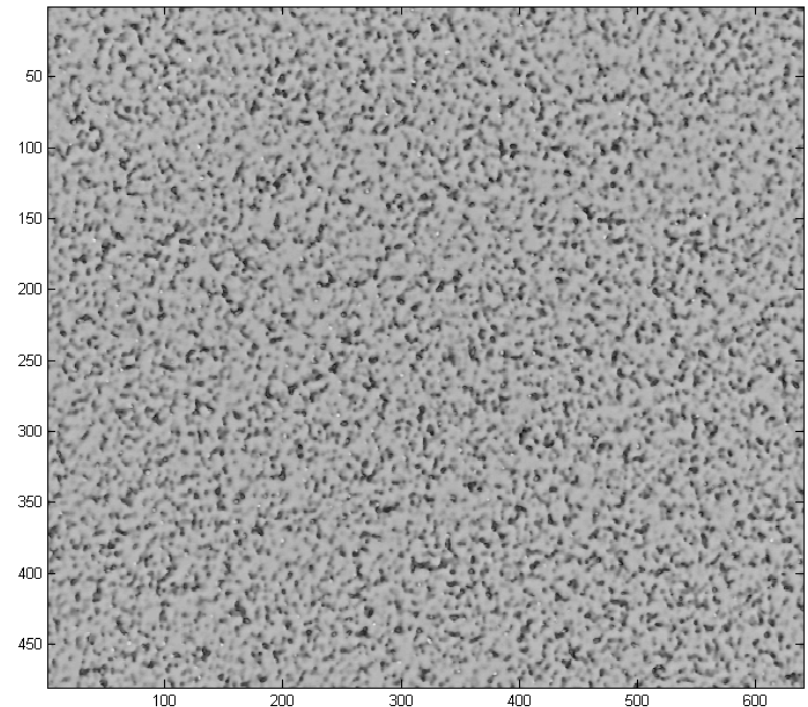
$$\rho = \sum_j q_j \int f_j(\mathbf{x}, \mathbf{p}, t) d\mathbf{p}$$

$$\mathbf{J} = \sum_j \frac{q_j}{m_j} \int \mathbf{p} f_j(\mathbf{x}, \mathbf{v}, t) d\mathbf{p}$$

# D1 protons >1MeV

- Distribution relatively uniform.
- Counts (based on 30 images) > 2E5 protons/mm<sup>2</sup>
- Total counts is 10<sup>8</sup> protons

FOV is 100um



# D3 proton $> 20$ MeV

- Highly non-uniform (bunch)
- Counts (average 30 images) :  $10^5$  protons/mm<sup>2</sup>
- Total count  $\sim 10^6$

FOV is 100um

